

See discussions, stats, and author profiles for this publication at: <https://www.researchgate.net/publication/235415318>

Optimal synthesis of double-phase computer generated holograms using a phase-only spatial light modulator with grating filter

Article in *Optics Express* · December 2012

DOI: 10.1364/OE.20.029844 · Source: PubMed

CITATIONS

62

READS

205

6 authors, including:



Sujin Choi
Eastern University

12 PUBLICATIONS 136 CITATIONS

[SEE PROFILE](#)



Kanghee Won
University of Cambridge

22 PUBLICATIONS 183 CITATIONS

[SEE PROFILE](#)



Hong-Seok Lee
SAIT, Samsung Electronics Co., Ltd.

96 PUBLICATIONS 941 CITATIONS

[SEE PROFILE](#)



Hwi Kim
Korea University

195 PUBLICATIONS 3,901 CITATIONS

[SEE PROFILE](#)

Optimal synthesis of double-phase computer generated holograms using a phase-only spatial light modulator with grating filter

Hoon Song,¹ Geeyoung Sung,¹ Sujin Choi,² Kanghee Won,¹ Hong-Seok Lee,¹ and Hwi Kim^{2,*}

¹*Samsung Advanced Institute of Technology (SAIT), South Korea*

²*Department of Electronics and Information Engineering, College of Science and Technology, Korea University, Sejong Campus, Sejong-ro 2511, Sejong 339-700, South Korea*
hwikim@korea.ac.kr

Abstract: We propose an optical system for synthesizing double-phase complex computer-generated holograms using a phase-only spatial light modulator and a phase grating filter. Two separated areas of the phase-only spatial light modulator are optically superposed by 4-*f* configuration with an optimally designed grating filter to synthesize arbitrary complex optical field distributions. The tolerances related to misalignment factors are analyzed, and the optimal synthesis method of double-phase computer-generated holograms is described.

©2013 Optical Society of America

OCIS codes: (230.6120) Spatial light modulators; (090.2870) Holographic display; (230.3720) Liquid-crystal devices; (120.5060) Phase modulation.

References and links

1. B. R. Brown and A. W. Lohmann, "Computer-generated binary holograms," *IBM J. Res. Develop.* **13**(2), 160–168 (1969).
2. C. K. Hsueh and A. A. Sawchuk, "Computer-generated double-phase holograms," *Appl. Opt.* **17**(24), 3874–3883 (1978).
3. L. G. Neto, D. Roberge, and Y. Sheng, "Full-range, continuous, complex modulation by the use of two coupled-mode liquid-crystal televisions," *Appl. Opt.* **35**(23), 4567–4576 (1996).
4. C. Slinger, C. Cameron, and M. Stanley, "Computer-generated holography as a generic display technology," *IEEE. Computer* **38**(8), 46–53 (2005).
5. S. Reichelt, R. Häussler, G. Fütterer, N. Leister, H. Kato, N. Usukura, and Y. Kanbayashi, "Full-range, complex spatial light modulator for real-time holography," *Opt. Lett.* **37**(11), 1955–1957 (2012).
6. E. Ulusoy, L. Onural, and H. M. Ozaktas, "Full-complex amplitude modulation with binary spatial light modulators," *J. Opt. Soc. Am. A* **28**(11), 2310–2321 (2011).
7. V. Arrizón, "Complex modulation with a twisted-nematic liquid-crystal spatial light modulator: double-pixel approach," *Opt. Lett.* **28**(15), 1359–1361 (2003).
8. M. M. M. Makowski, A. S. A. Siemion, I. D. I. Ducin, K. K. K. Kakarenko, M. S. M. Sypek, A. M. S. A. M. Siemion, J. S. J. Suszek, D. W. D. Wojnowski, Z. J. Z. Jaroszewicz, and A. K. A. Kolodziejczyk, "Complex light modulation for lensless image projection," *Chin. Opt. Lett.* **9**(12), 120008 (2011).
9. J.-P. Liu, W.-Y. Hsieh, T.-C. Poon, and P. Tsang, "Complex Fresnel Hologram Display using a Single SLM," *Appl. Opt.* **50**(34), H128–H135 (2011).
10. H. Kim and B. Lee, "Analytic design of an anamorphic optical system for generation anisotropic partially coherent Gaussian Schell-model beams," *Opt. Commun.* **260**(2), 383–397 (2006).
11. H. Kim, J. Hahn, and B. Lee, "Mathematical modeling of triangle-mesh-modeled three-dimensional surface objects for digital holography," *Appl. Opt.* **47**(19), D117–D127 (2008).

1. Introduction

Complex spatial light field modulation technology using spatial light modulators (SLMs) has been actively researched since the beginning of digital holography [1–3]. But the necessity of complex SLM has not been as strong as in recent years with the global onset of genuine investment in the research and development of holographic three-dimensional (3D) displays. Holographic 3D displays are considered as the next-generation or ultimate 3D display, providing the most natural and satisfactory 3D scenes. The research and development of holographic 3D displays has advanced in accelerating steps [4].

The most challenging technology for realizing holographic 3D displays is the complex spatial light modulator with wavelength-scale pixel size and ultra-high resolution. In principle, given independently controllable and very thin amplitude and 2π -range phase modulation SLMs, we can realize perfect complex SLMs by cascading the two SLMs with precision pixel matching alignment [3]. However, in practice, the cascading architecture suffers from many practical problems, including serious cross-talk due to diffraction during the long-distance propagation of an optical field. A second practical problem is the fine alignment of two distant phase- and amplitude-type SLMs to pixel-to-pixel matching level. Serious Moiré patterns can be generated due to a slight misalignment. To avoid these problems, several alternative methods using a single SLM have been developed [2, 5–9]. The double-phase hologram (DPH) or two-phase encoding method is one of the most practical candidates for complex SLM [2, 5, 7]. Basically, the DPH is an interferometric technique conveying two separated computer-generated phase holograms, which are combined to produce a computer-generated complex optical field, referred to as a double-phase computer-generated hologram (DPCGH). Recently, an advance in the DPH technique has been reported, wherein a polarization sensitive component (PSC) and a polarizer were used to combine two adjacent phase-only pixels within a short distance enabling neglect of the diffraction effect on the complex modulation [5]. This DPH architecture is encouraging, since the thickness of the architecture can be reduced to ignore the diffraction effect by using two adjacent pixels in a single panel. For this, the beam-combining optics composed of thin optical films was invented. However, the PSC element and polarizer are not cost-effective and it is not easy to make large size complex SLMs due to the practical limitation in scaling the PSC element.

These previous works have inspired a basic question regarding the possibility of making a DPH configuration using cost-effective non-polarization elements, and a strong need for investigation of the design and analysis of bulk-optic DPH systems and compact device-level DPH architectures. Recently, optical systems using binary diffraction grating for synthesizing an optical complex field has been reported, combining the real and imaginary terms based on the concept of optical scanning holography [9]. In this paper, a similar configuration with diffraction grating is used to design DPH systems for generating complex optical fields. Because of its interferometric properties, the DPH system is sensitive to misalignment and aberration of the optical system. The noise inherent in the DPH has not been a central issue in complex optical field synthesis, but our analysis shows that the effect of the translation mismatch and long propagation diffraction is profoundly influential on the imaging quality of holographic 3D images displayed by the DPH system. We propose a DPH system using a phase-only SLM with a grating filter, and analyze the intriguing degradation effect observed in the proposed DPH system associated with misalignment and diffraction, and its physical mechanism. Based on the analysis, we describe the optimal encoding method for the DPH system.

In section 2, two comparative DPH configurations using a phase-only SLM and a grating filter are proposed and modeled mathematically. In section 3, the performance of the DPH systems is analyzed numerically, which is followed by the conclusion.

2. Two double-phase hologram configurations

To study the DPH system, we set up two DPH configurations based on a spherical $4-f$ optical system and a cylindrical $4-f$ optical system with a grating filter inserted in the Fourier domain, as illustrated in Figs. 1(a) and 1(b), respectively. A plane wave is normally incident on the phase-only SLM in the input plane, where two phase holograms, $\exp(j\Theta_{up})$ and $\exp(j\Theta_{low})$, i.e. DPH, are displayed in symmetrically separated regions, where the double slit aperture isolates the phase hologram regions clearly. The DPH is imaged in the output plane through the spherical or the x -axis cylindrical $4-f$ system with a periodic grating filter inserted in the Fourier filter plane. The role of the grating filter is bidirectional translation of the SLM image along the $\pm x$ -axis directions in the output plane by diffractive beam splitting,

which leads to coherent superposition of the upper and lower phase holograms in the overlapped region in the center of the output plane [9]. The phase-hologram images can be transferred through higher-order diffraction channels and contaminates the output field, as shown in Fig. 1(a), but these signals can be rejected simply by an opaque spatial filtering mask.

In the configuration using spherical lenses, the 4- f system is constructed for both x - and y -directions. Under the ideal alignment condition, the accurate overlapping imaging of the DPH can be obtained, and as a result, the formation of a nearly perfect complex optical field is expected to be synthesized in the output plane of the 4- f system. We will analyze the influence of the misalignment of the upper and lower phase holograms in the output plane and the vertical shift of the grating filter for the generation of holographic 3D images, and address the conditions for optimal performance of the system.

To obtain additional insight on the effect induced by diffraction, the modified 4- f DPH system with cylindrical lenses shown in Fig. 1(b) is examined comparatively. In the cylindrical 4- f system, the two-dimensional optical transform of the system is separated by x - and y -dependent 1D transforms. For the x -direction, the 1D 4- f system is realized, but for the y -direction, the system looks like 1D free space to the propagating optical field, and as a result, the y -directional 1D Fresnel diffraction image of the DPH is formed in the output plane. In theory, the Fresnel diffraction can be viewed as the multiplication of the quadratic phase term or propagator function to the angular spectrum of the optical field, where the phase profile of the propagator function becomes highly oscillating in proportion to the propagation distance, meaning the Fresnel diffraction makes the phase profile structure of the optical field more complicated.

The quadratic phase provided by the lens compensates for the diffractive divergence of an optical field through inter-distant free-space. By intentionally eliminating this quadratic phase compensation by using a cylindrical configuration, we can understand the diffraction effect on complex optical field synthesis more analytically. The grating filter in the Fourier domain plays the same role of copying the resultant DPH images periodically in the output plane. Under perfect alignment condition, the \pm first-order images are coherently overlapped in the central region to produce a designed complex optical field or complex CGH. In this configuration, we would like to figure out the effect of the 1D Fresnel diffraction on the misalignment tolerance and degradation of synthesized holographic 3D images.

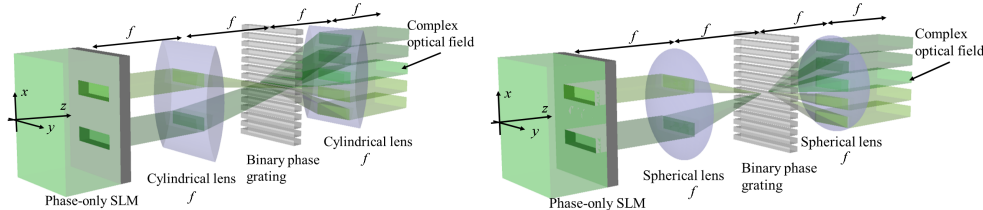


Fig. 1. DPH configurations of synthesizing complex optical field based on (a) spherical 4- f system with grating filter and (b) cylindrical 4- f system with grating filter

The spherical 4 f system with a grating filter inserted in the Fourier domain can be mathematically modeled based on Fourier optics theory [10]. The system is divided into the first part in front of the grating plane and the second part behind the grating plane. The spherical and cylindrical 4- f systems are represented by the generalized Fresnel transform with separable kernel [10]. The generalized Fresnel transform between the input plane (x_1, y_1) and the output plane (x_2, y_2) is described by the following forward generalized Fresnel integral transform

$$G(x_2, y_2) = \int_{-\infty}^{\infty} h_y(y_2, y_1) \left[\int_{-\infty}^{\infty} h_x(x_2, x_1) F(x_1, y_1) dx_1 \right] dy_1, \quad (1a)$$

where the input and the output fields are denoted by $F(x_1, y_1)$ and $G(x_2, y_2)$, respectively, and the x -dependent kernel $h_x(x_2, x_1)$ is given, for the spherical and cylindrical systems, by

$$h_x(x_2, x_1) = (\lambda f)^{-1/2} e^{-j\pi/4} \exp[-j2\pi x_1 x_2 / (\lambda f)], \quad (1b)$$

and the y -dependent kernel $h_y(y_2, y_1)$ is given, for the spherical and cylindrical systems, respectively, by

$$h_y(y_2, y_1) = (\lambda f)^{-1} e^{-j\pi/4} \exp[-j2\pi y_1 y_2 / (\lambda f)], \quad (1c)$$

and

$$h_y(x_2, x_1) = (2\lambda f)^{-1} e^{-j\pi/4} \exp[j\pi\{y_1^2 - 2y_1 y_2 + y_2^2\} / (2\lambda f)], \quad (1d)$$

where λ and f are the wavelength and focal length of the lenses, respectively. To calculate the DPCGH, we need to define the inverse generalized Fresnel transform as

$$F(x_1, y_1) = \int_{-\infty}^{\infty} h_y^{-1}(y_1, y_2) \left[\int_{-\infty}^{\infty} h_x^{-1}(x_1, x_2) G(x_2, y_2) dx_2 \right] dy_2, \quad (2a)$$

where the x -dependent inverse kernel $h_x^{-1}(x_1, x_2)$ is given, for the spherical and cylindrical systems by

$$h_x^{-1}(x_2, x_1) = (\lambda f)^{-1} e^{j\pi/4} \exp[j2\pi x_2 x_1 / (\lambda f)], \quad (2b)$$

and the y -dependent inverse kernel $h_y^{-1}(y_2, y_1)$ is given, for the spherical and cylindrical systems, respectively, by

$$h_y^{-1}(y_2, y_1) = (\lambda f)^{-1} e^{j\pi/4} \exp[j2\pi y_2 y_1 / (\lambda f)], \quad (2c)$$

and

$$h_y^{-1}(y_2, y_1) = (2\lambda f)^{-1/2} e^{j\pi/4} \exp[-j\pi\{y_1^2 - 2y_1 y_2 + y_2^2\} / (2\lambda f)]. \quad (2d)$$

In the case of the spherical $4f$ system, the transform kernel of the first part is given by the multiplication of Eqs. (1b) and (1c). The optical field in the Fourier domain (grating plane) is multiplied by the transmittance function of the grating filter. The optical field modulated by the grating filter is transmitted to the output plane through the second part, which has the same composition as the first part. In the inverse transform of Eq. (2a), the multiplication of the grating transmittance function should be omitted, where the inverse kernel is composed of Eqs. (2b) and (2c). In the case of the cylindrical $4f$ system, the transform kernel of the first and second parts is the multiplication of Eqs. (1b) and (1d), and the corresponding inverse kernel is composed of Eqs. (2b) and (2d). Therefore, the total forward and inverse transformations used in the modeling of the DPH systems are respectively represented as

$$G = \left\{ H_y \cdot H_x \left[t_{GR} \left\{ H_y \cdot H_x [F] \right\} \right] \right\}, \quad (3a)$$

and

$$F = \left\{ H_y^{-1} \cdot H_x^{-1} \left[\left\{ H_y^{-1} \cdot H_x^{-1} [G] \right\} \right] \right\}, \quad (3b)$$

where $H_{x(y)}[F]$ and $H_{x(y)}^{-1}[F]$ represents the 1D integral transform of F with kernel $h_{x(y)}$ and its inverse transform, and $H_y \cdot H_x[F]$ is the cascaded application of the integral transforms H_x and H_y to F and t_{GR} is the transmittance function of the grating filter.

Let the target complex optical field be denoted by $G(x, y)$. Then the inverse generalized Fresnel transform of G is performed to obtain the DPH as

$$A \exp(j\Phi) = \left\{ h_y^{-1} \cdot h_x^{-1} \left[\left\{ h_y^{-1} \cdot h_x^{-1} [G] \right\} \right] \right\}. \quad (4a)$$

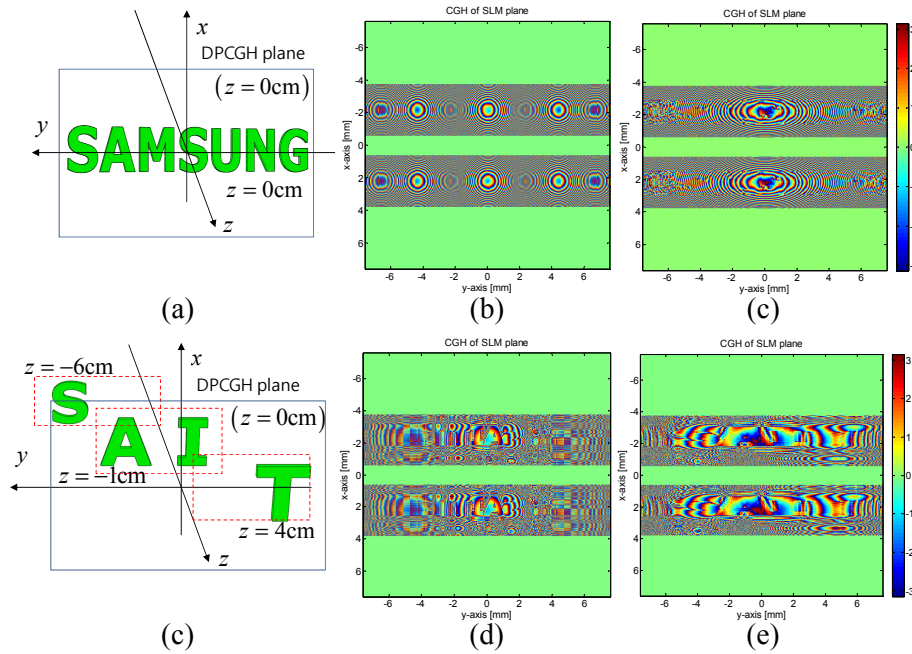


Fig. 2. (a) 2D target image 'SAMSUNG' and its DPH for (b) the spherical 4-f system, and (c) the cylindrical 4-f system. (d) 3D target image 'SAIT' and its DPHs for (e) the spherical 4-f system and (f) the cylindrical 4-f system.

In particular, when the target image includes zero intensity in its signal domain, the inverse transform of Eq. (4a) can induce random noise in the zero intensity region of the reconstructed image since the phase cannot be properly determined in the zero-intensity points. To prevent this undesired random noise, which can deteriorate the signal-to-noise ratio, we employ a small positive regularization constant δ in the inverse transform Eq. (4a) in the following form

$$A \exp(j\Phi) = \left\{ h_y^{-1} \cdot h_x^{-1} \left[\left\{ h_y^{-1} \cdot h_x^{-1} [G + \delta] \right\} \right] \right\}. \quad (4b)$$

The complex optical field in the input DPH plane (SLM plane), $A_\delta \exp(j\Phi_\delta)$, can be represented as the sum of two pure phase functions with constant amplitude as

$$A \exp(j\Phi) = \frac{1}{2} \exp[j(\Phi + \psi)] + \frac{1}{2} \exp[j(\Phi - \psi)], \quad (5)$$

where $\psi = \arccos A$ and $0 \leq \psi \leq \pi/2$. The upper and lower holograms, $\exp(j\Theta_{up})$ and $\exp(j\Theta_{low})$, are given, respectively, by

$$\exp(j\Theta_{up}) = \exp[j(\Phi + \psi)], \quad (6a)$$

and

$$\exp(j\Theta_{low}) = \exp[j(\Phi - \psi)]. \quad (6b)$$

In the numerical simulation of the DPH system, the upper and lower phase holograms are assumed to have the x -directional width, $w = 3.2\text{mm}$ and the x -directional shift of the center of the upper area from the origin ($x = 0\text{mm}$) is set to $d = 2.2\text{mm}$. The grating period (Λ) is determined such that the first-order diffraction of a normally directed optical ray passing the center of the upper or lower phase hologram and heading toward the center of the grating filter is exactly aligned to the normal direction parallel to the z -directional optic axis. In this sense, the grating period, Λ , is given by $\Lambda = \lambda\sqrt{f^2 + d^2}/d$. In the simulation, Λ is set to $36.8\mu\text{m}$ for $f = 15\text{cm}$ and $d = 2.2\text{mm}$ and the fill-factor of the grating filter is chosen as 0.5 for convenience. In Fig. 2, the DPHs for two comparative complex field syntheses of the 2D target image ‘SAMSUNG’ and 3D target image ‘SAIT’ are presented. Figures 2(b) and 2(c) are the DPHs of ‘SAMSUNG’ for the spherical and cylindrical $4f$ systems, respectively, and those for ‘SAIT’ are shown in Figs. 2(e) and 2(f), respectively. The second example ‘SAIT’ is dressed with a spherical phase profile to be correctly observed by a virtual camera with a 1cm-radius aperture located at $z = 1\text{m}$. The observation of the accommodation effect of the holographic 3D image ‘SAIT’ is presented and discussed in the next section.

3. Comparison of the complex field synthesis by two DPH configurations

In this section, the performance and tolerance of complex field synthesis of the spherical and cylindrical DPH configurations are comparatively analyzed. Our focus of analysis is on the tolerance of the translation mismatch of two phase holograms at the output plane and the vertical spatial shift of the grating filter, which are denoted by Δd and Δh , respectively. For quantitative analysis, the image quality measure of the obtained complex field, $F(x, y)$, i.e., a holographic image, is defined by the signal-to-noise ratio (SNR) in the form of

$$SNR = \iint_S |F(x, y)|^2 dx dy / \left\{ \iint_S |F(x, y)|^2 dx dy + \iint_N |F(x, y)|^2 dx dy \right\}, \quad (7)$$

where S and N indicate signal and noise areas in the output plane, respectively. The definition of SNR is appropriate for the evaluation of 2D optical field distribution, but a more sophisticatedly designed measure for quantitatively scoring the quality of holographic 3D image has to be investigated further. Here, the SNR measure of Eq. (7) is only used to evaluate the image quality of the first synthesis example of the ‘SAMSUNG’ 2D flat image in the output plane. As will be discussed in this section, the SNR analysis is used to analyze the influence of the system parameters, Δd and Δh on the formation of ‘SAMSUNG’.

The phase holograms of Eqs. (6a) and (6b) are displayed in the upper and lower regions of the SLM, respectively, as shown in Fig. 2. Let us pose a misalignment problem as follows. The misaligned DPH function is defined as

$$M(x, y; \Delta d) = \Gamma(x - d)e^{j\Theta_{up}(x-d, y)} + \Gamma(x + d + \Delta d)e^{j\Theta_{down}(x+d+\Delta d, y)}, \quad (8a)$$

where $\Gamma(x)$ is the rectangular aperture given as $\Gamma(x) = \text{rect}(x/w)$. Also, in a practical system, the vertical (x -directional) shift of the grating filter, Δh , is inevitable, which induces

a phase difference between the positive and negative first-order diffraction fields. This phase difference significantly impacts the interference of the DPCGH, and the compensating factor phase compensation factor, $\Delta\theta$, must be considered. This phase compensation factor for the grating shift is inserted by the addition of a constant phase to the lower phase hologram, and the resulting expression of the misaligned DPH takes the form of

$$M(x, y; \Delta d, \Delta\theta) = \frac{1}{2} \Gamma(x-d) e^{j\Theta_{up}(x-d, y)} + \frac{1}{2} \Gamma(x+d+\Delta d) e^{j\Theta_{low}(x+d+\Delta d, y)} e^{j\Delta\theta}. \quad (8b)$$

The synthesized complex optical field, \bar{F} , of the misaligned DPH, $M(x, y; \Delta d, \Delta\theta)$, is obtained by the forward generated Fresnel transform,

$$\bar{F} = \left\{ h_y \cdot h_x \left[t_{GR} \left\{ h_y \cdot h_x [M] \right\} \right] \right\}. \quad (9a)$$

In this study, the use of an ideal sinusoidal grating filter and a binary-phase grating that is an approximation of the ideal sinusoidal grating filter are compared. The grating transmittance functions, t_{GR} for the former and latter cases are given, respectively, as

$$t_{GR}(x) = \cos(2\pi x / \Lambda), \quad (9b)$$

and

$$t_{GR}(x) = \text{sgn}(\cos(2\pi x / \Lambda)), \quad (9c)$$

where $\text{sgn}(a)$ is the sign function that indicates 1 or -1 according to whether the real number a is positive or negative. In practice, the sinusoidal grating profile has a negative and positive gray scale amplitude profile, which requires a composite structure of binary phase and gray scale amplitude modulation layers, while the binary grating can be simply fabricated by a periodic surface relief structure on transparent substrate, so the use of binary phase grating is practical. However, from a theoretical point of view, the comparison of two types of grating filters is valuable to understand the theoretical limit of the synthesis performance.

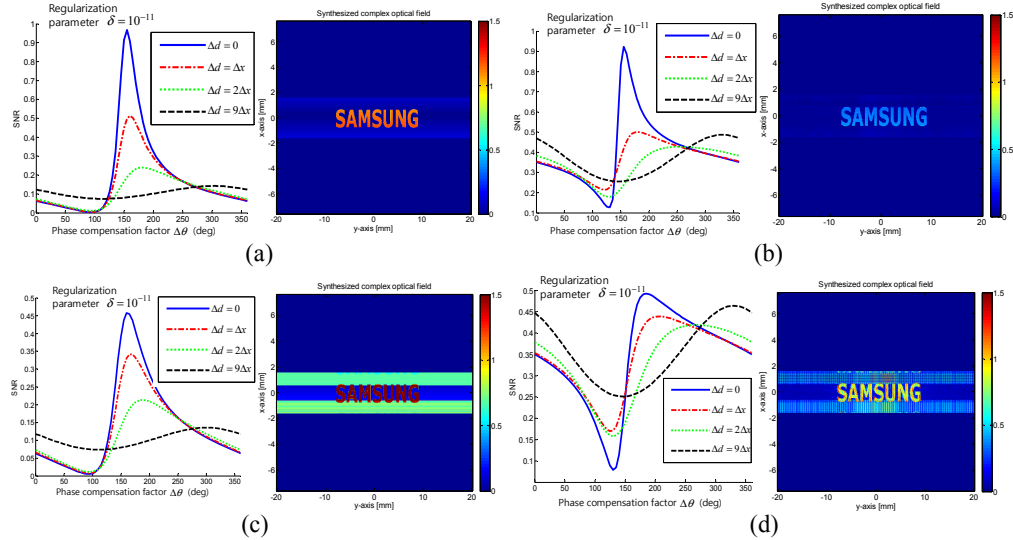


Fig. 3. SNR variations for the misalignment factors in the cases of (a) spherical 4- f system with sinusoidal grating, (b) cylindrical 4- f system with sinusoidal grating, (c) spherical 4- f system with binary grating, and (d) cylindrical 4- f system with binary grating.

In Fig. 3, the SNR variations for the misalignment factors, Δd and $\Delta\theta$, are compared for four different DPH system configurations; (i) spherical 4- f system with sinusoidal grating filter, (ii) cylindrical 4- f system with sinusoidal grating filter, (iii) spherical 4- f system with binary grating filter, and (iv) cylindrical 4- f system with binary grating filter. The maximum peak SNR indicates the optimal phase compensation parameter for specified translation misalignment of DPH. In the analysis, the SNR versus $\Delta\theta$ for $\Delta d = 0$, $\Delta d = \Delta x$, $\Delta d = 2\Delta x$, and $\Delta d = 9\Delta x$ are compared, where Δx is set to $8\mu\text{m}$, which is the pixel size of a conventional phase-only SLM (PLUTO made by the HoloEye corporation). The regularization parameter δ is set to 10^{-11} . In the case of perfect alignment of DPH with $\Delta d = 0$, the optimal $\Delta\theta$ for the four cases, (i)-(iv), are obtained as 155(deg), 155(deg), 160(deg), and 185(deg), respectively.

The optimal $\Delta\theta$ is dependent on the 3D object image itself as well as the position of the grating filter. As seen in Eq. (8b), the finite-size rectangular window function $\Gamma(x)$ restricts the bandwidth of the holograms. When the light field representing the object image has wide angular spectral bandwidth, the high spatial-frequency components are rejected by the finite band-limiting window, $\Gamma(x)$. This operation can modify the original light field profiles. The obtainable complex light field at the DPCGH plane is the superposition of two light fields modulated by the phase-holograms with limited bandwidth. In this case, the light field matching condition is deviated from the mathematically exact condition. The background noise pattern is sensitive to the field modification since the background noise has faster oscillating features (high spatial frequency components) than the image signal. Thus the noise terms in the complex light fields generated by the upper and lower holograms lose the mathematically deterministic property, thus two light fields from two holograms $\exp(j\Theta_{up})$ and $\exp(j\Theta_{low})$, should be considered as having totally independent degrees of freedom. Therefore the phase compensation factor $\Delta\theta$ should be statistically determined by the way of minimizing the average errors and maximizing the SLR as presented in the analysis of Fig. 3. Also, in practical experiments, the optimal compensation factor $\Delta\theta$ should be extracted by parametric searching.

Comparing the obtained reconstructed images of ‘SAMSUNG’, the SNRs of both the spherical and cylindrical system with a sinusoidal grating filter reach a nearly perfect value of 1, as shown in Figs. 3(a) and 3(b). But under the optimal SNR condition, the absolute amplitude of the reconstructed image, and relative diffraction efficiency, of the spherical system are much greater than that those of the cylindrical lens system. The distinguishable point of the spherical system from the cylindrical system is the higher diffraction efficiency. However, it is also noteworthy that the SNR over 90% (0.9) is obtainable by the cylindrical 4- f configuration, although the diffraction efficiency is relatively low. The use of binary grating is a practical choice, but the 0th order noise and higher-order stray noise are significant in the background of the obtained reconstructed images as indicated in Figs. 3(c) and 3(d) even in the optimal SNR condition. The maximum SNR is smaller than 50% (0.5), which poses a limitation of the image quality achieved using binary phase grating. The diffraction efficiency of the cylindrical 4- f configuration is relatively lower than that of the spherical 4- f system, which is similar to the case of the system with a sinusoidal grating filter.

In Fig. 4, the 3D observation simulation [11] of the holographic 3D images through the DPH configurations (i)-(iv) is performed for the 3D target image ‘SAIT’ shown in Fig. 2(d). The letters ‘S’, ‘AI’, and ‘T’ are located in the transversal planes at $z = -6\text{cm}$, $z = -1\text{cm}$, and $z = 4\text{cm}$, respectively. As shown in Fig. 4, all configurations generate clear accommodation effects in observations. The comparison of the noise distribution between the systems with sinusoidal grating and binary grating filters confirms the superiority of using the sinusoidal grating. Comparing the observed images, we can see that the quality of the cylindrical 4- f image is comparable to that of the spherical 4- f system with respect to noise

distribution, but its diffraction efficiency seems to be lower than that of the spherical $4-f$ system.

The analysis shows that the amount of noise and its vulnerability to misalignment around a specified position are related to the local oscillation frequency in the phase structure of DPCGH, which tends to be more oscillatory as a corresponding target object moves far away from the DPCGH plane (the output plane) as seen from a comparison of Figs. 2(b) and 2(e), and Figs. 2(c) and 2(f). As the phase profile has highly oscillating features, a slight misalignment leads to catastrophic destruction of the DPCGH pattern, which is the origin of degradation and noise that are expected in practical experiments. In practice, the expressible 3D depth is limited due to the vulnerability to misalignment as well as expressible spatial frequency in the DPH system. The adaptation of the small positive number δ for regularization is to reduce the randomly distributed noise by enhancing the phase regularity of DPCGH.

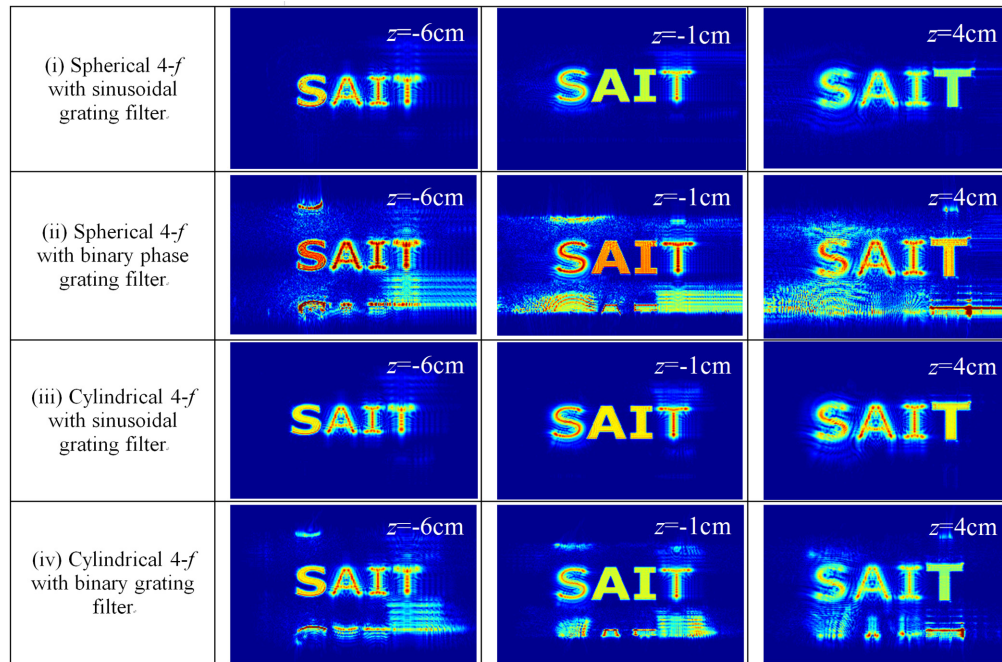


Fig. 4. Observation of holographic 3D images generated by the spherical $4-f$ system with (a) sinusoidal grating filter and (b) binary phase grating filter, and cylindrical $4-f$ system with (c) sinusoidal grating and (d) binary phase grating.

From a practical point of view, the cylindrical $4-f$ system is advantageous in the minimization and scalability of fabrication in the form of arrays. The configurations shown in Figs. 1(a) and 1(b) are the bulky optical system, where the SLM is supposed to have phase holograms composed of a large number of pixels. Within the total axial length, the y -directional Fresnel diffraction for the cylindrical $4-f$ system is considerable. For the downsizing of the system to the device level, wherein the SLM component only represents adjacent two pixels on a micrometer scale, the cylindrical $4-f$ configuration is more acceptable than the spherical $4-f$ configuration, since a cylindrical lens array is easier to fabricate than a spherical lens array.

As discussed, the use of an ideal sinusoidal grating with positive and negative amplitudes for the configurations produces the optimal performance of synthesizing a complex light field by eliminating the 0th order noise and higher stray diffractions. However, the reduction of the axial length of the optical system is expected to enable us to adjust the grating period to eliminate the images brought through higher diffraction channels. Also, although the

sinusoidal grating is essential for maximizing the SNR and displaying complex DPCGH images clearly, its total transmission efficiency is 50% and the even splitting of the 50% optical power results in the eventual diffraction efficiency limitation of 25% in synthesizing DPCGH. The total transmission efficiency of the sinusoidal grating is 25%. However, the maximum achievable efficiency of the system using the binary phase grating is dated to about 40%, since the usual binary phase gratings can be optimized to have maximum diffraction efficiency of about 80%. The high diffraction efficiency of the binary phase grating can be an appealing point with regard to practical device implementation. Therefore, it is reasonable that the cylindrical lens configuration with a binary grating can be adopted as a candidate for complex SLM device architecture based on two-pixel combination as well as general complex field synthesis based on the bulk optic system configuration. It is expected that the diffraction effect is reduced for short inter-distance between the panel and the output plane in device-level architecture.

4. Conclusion

We have investigated and analyzed the optical performance of DPH configurations based on $4-f$ configuration with grating filters, and addressed the optimization method of the system parameters associated with misalignment. It has been shown that two separated phase holograms on a single phase-only SLM can be effectively combined with simple cylindrical $4-f$ configuration with a binary phase grating filter, to generate the desired complex optical field that can yield correct holographic 3D images. This scheme is the most practical and feasible scheme for device fabrication. The next step is to design a realizable device-level architecture of DPH using cost-effective and scalable elements, such as lens arrays and phase gratings, without using expensive and non-scalable polarization sensitive devices. In the same direction, we will further investigate more simplified device structure without using lenses.

Acknowledgment

This work is supported by the IT R&D program of the MKE/KEIT [KI001810039169, Development of Core Technologies for Digital Holographic 3D Display and Printing System].